JAAS

Journal of Analytical Atomic Spectrometry

Accepted Manuscript

JAAS

Journal of Analytical Atomic Spectrometry

rsc.li/jaas

Volume 32
Number 1
January 2017
Pages 1-202

ISSN 0267-9577

ROYAL SOCIETY OF CHEMISTRY

PAPER
José-Luis Todolí *et al.*
Analysis of whole blood by ICP-MS equipped with a high temperature total sample consumption system

ROYAL SOCIETY OF CHEMISTRY

rsc.li/jaas

Innovations in Battery Material Quality Control: Microwave-Induced Atmospheric-Pressure Plasma Optical Emission Spectrometry (MICAP-OES) for Elemental Analysis

Jorge Pérez, Raquel Serrano, Guillermo Grindlay, Luis Gras, Juan Mora

Department of Analytical Chemistry, Nutrition and Food Sciences, University of Alicante, PO Box 99, 03080 Alicante, Spain.

E-mail: Raquel.serrano@ua.es

Abstract

The analysis of both, major elements (Li, Ni, Co, Mn) and impurities (e.g., Ca, Cd, Cr, Cu, Fe, Na, Pb) in final cathodes and especially in raw materials is essential for quality control in Li-based batteries industry. In recent years, Microwave-Induced Atmospheric-Pressure Plasma Optical Emission Spectrometry (MICAP-OES) has emerged as a robust analytical technique for trace element determination, even in complex matrices with high concentration of total dissolved solids. Thus, the aim of this study is to evaluate the analytical capabilities of MICAP-OES for quality control purposes (major and impurities determination) in different materials used in Li-based battery industry (i.e., raw materials and cathodes) in accordance with the current Chinese standard protocols. Despite the complexity of the samples, no significant spectral interferences were detected for the most sensitive wavelength of analytes, except in the case of Pb which is interfered in Mn-containing matrices. With regard to

non-spectral interferences, although the method is still susceptible to matrix effects caused by sample concomitants (mainly Li), these can be effectively corrected using matrix-matched calibration standards. Furthermore, with the appropriate selection of operating conditions and the calibration strategies, both major elements and impurities can be determined simultaneously. The detection limits achieved are comparable to those afforded by ICP-OES, and allow the analysis of impurities according to the Chinese standard protocols. Finally, the proposed methodology was satisfactorily validated through the analysis of a cathode reference material (NMC 111 BAM S014), 5 commercial raw materials and 9 cathode samples with different composition.

Keywords:

Microwave plasma, optical emission spectrometry, raw materials, cathodes, quality control

1. Introduction

In recent years, the demand for high-capacity electrochemical power sources with long lifetimes has grown. This is due to the rapid increase in the use of electronic mobile devices (e.g. smartphones, tablets, laptops, etc.), and the development of new pure and hybrid electric vehicles.[1] The ongoing advancement of lithium-ion batteries (LiBs), coupled with the substantial research conducted on their constituent materials, has firmly established this particular battery type as a frontrunner within the energy sector.[2] Amongst all variants of LiBs (e.g., lithium cobalt batteries, lithium-iron phosphate batteries, etc.), those containing a ternary cathode (NMC) ($LiNi_xMn_yCo_{(1-x-y)}O_2$) have become one of the

most commonly used in recent times due to their high capacity, good cycle stability (battery life) and moderate cost.[3] The stoichiometry in which the main elements (i.e., Li, Ni, Co, Mn, Fe, etc.) are found in the different cathode materials can significantly affect the performance and cost of the LiBs. Additionally, the presence of some impurities (i.e., Al, Ca, Cd, Cr, Cu, Fe, Mg, Na, Pb, Zn) in the cathode materials plays an important role in the production of them. Consequently, the accurate determination and precise quantification of the primary elements (i.e., Li, Mn, Co, Ni, Al), in conjunction with the meticulous control of trace impurities in both the starting materials (e.g., $CoSO_4 \cdot 7\,H_2O$, $FePO_4 \cdot 2\,H_2O$, Li_2CO_3, $LiOH \cdot H_2O$, $MnSO_4 \cdot H_2O$, $NiSO_4 \cdot 6\,H_2O$), intermediates and the finished products, becomes particularly important.[4] Indeed, China, as the main global LiBs manufacturers, has developed the only regulatory standards protocols available to date to ensure the quality control of the raw materials employed for cathode production (YS/T 582-2023 (Li_2CO_3)[5], GB/T 26008-2020 (LiOH)[6], HG/T 5918-2021 ($CoSO_4 \cdot 7\,H_2O$)[7], HG/T 4823-2015 ($MnSO_4 \cdot H_2O$)[8], HG/T 5919-2021 ($NiSO_4 \cdot 6\,H_2O$)[9], HG/T 4701-2021 ($FePO_4 \cdot 2\,H_2O$)[10]), and to regulate the stoichiometry of the main elements and the impurities in the final cathode materials (YS/T 798-2012 (NMC)[11], GB/T 20252-2014 (LCO)[12], YS/T 1027-2015 (LFP)[13], GB/T 37202-2018 (LNMO)[14], YS/T 677-2016 (LMO)[15], YS/T 1125-2016 (NCA)[16]).

Elemental analysis of LiBs raw materials and cathodes is performed by means inductively coupled plasma optical emission spectrometry (ICP-OES) and inductively coupled plasma mass spectrometry (ICP-MS) due to their multi-elemental capabilities, sample throughput and detection limits at trace and ultra-

trace levels. Nevertheless, because of the high concentrations of easily ionizable elements, such as Li, and some transition metals (Co, Fe, Mn, and Ni), both spectral and non-spectral interferences might arise hindering the accurate quantification of impurities. For this reason, several strategies have been proposed in the literature to mitigate these interferences for analysing impurities in various LiBs materials (i.e., $LiPF_6$ electrolyte, $LiFePO_4$ (LFP), lithium cobalt oxide (LCO), NMC cathodes, Lithium materials (LiOH, Li_2CO_3)) by means of ICP-OES and ICP-MS using different strategies to avoid them such us: (i) different sample introduction systems (e.g., fully demountable extended matrix tolerance quartz torch, an argon humidifier, among others);[2,17] (ii) different calibration techniques (i.e., standard addition, matrix-matched standard calibration, internal standard addition, etc.);[18,19,20,21] and (iii) cell reaction in the case of ICP-MS using NH_3 or O_2 as reaction gases;[22] to minimize the matrix effects caused, by Li as the main component in LiBS.

In recent years, the high-power microwave induced plasmas (MIP) have emerged as a viable alternative to the elemental analysis, offering analytical performance comparable to ICP-OES.[23,24] However, to date, the use high-power MIP system in the analysis of LiBs remains almost unexplored. This fact may be attributable to the comparatively lower energetic plasmas (i.e., lower plasma temperatures) compared with ICP-OES, which results in more significant matrix effects especially when operating solutions with high content of easily ionization elements.[25,26] Only one study is known in which a high-power MIP has been used for the analysis of NiMH battery residues. In this study, Cruz et al.[27] reported quantitative values for the multi-element analysis of diluted sulfuric acid leachates

of NiMH battery residues by means of MIP-OES (i.e., Hammer cavity) employing a multi-energy calibration (MEC) strategy to mitigate matrix effects.

Within the recent progress made in MIPs, previous studies have demonstrated that Microwave-Induced Atmospheric-Pressure Plasma Optical Emission Spectrometry (MICAP-OES) provides a more stable discharge in comparison to other high-power MIP systems.[28,29] Indeed, MICAP-OES has been employed in the analysis of samples with diverse matrices, including saline solutions (i.e., 0.1 mol L^{-1} Na, 0.25 mol L^{-1} Ca, and 0.03 mol L^{-1} K), with positive results, which suggest that it could be a useful technique for the analysis of battery industry-related samples.[30,31] Thus, the aim of the present study is to evaluate the feasibility of MICAP-OES for the quality control (i.e., content of major elements and impurities) in raw materials employed for the production of LiBs and in different Li-based cathodes. To this end, spectral and non-spectral interferences were investigated for 36 emission lines of a total of 15 elements, corresponding to the major elements and the impurities regulated by the Chinese standard protocols for LiB materials (Al, B, Ca, Cd, Co, Cr, Cu, Fe, Li, Mg, Mn, Na, Ni, Pb and Zn) in the presence of different synthetic matrix solutions. Based on the results obtained in this study, optimal experimental conditions were selected to maximize detection capabilities and different calibration strategies were evaluated to mitigate matrix effects. Finally, the developed procedure was validated by analysing a cathode CRM (NMC111 BAM S014), 6 different raw materials (e.g., LiCO$_3$, LiOH, CoSO$_4$, MnSO$_4$, NiSO$_4$ and FePO$_4$) and 9 cathodes samples (e.g., lithium cobalt oxide, lithium iron phosphate, lithium manganese oxide, lithium nickel cobalt aluminium oxide, and 5 lithium nickel manganese

cobalt oxide cathodes with different stoichiometries).

2. Experimental

2.1 Reagents

All solutions were prepared using deionised water obtained from a Milli-Q purification system (Millipore, Paris, France). Suprapure nitric acid 69 % w w^{-1}, and hydrochloric acid 37 % w w^{-1} were obtained from Panreac (Barcelona, Spain). High-purity metal nitrates, including cobalt (II) nitrate tetrahydrate (98%), iron (III) nitrate nonahydrate (99.0%), manganese (II) nitrate tetrahydrate (98.5%), and nickel (II) nitrate hexahydrate (98%), were purchased from Scharlau (Valencia, Spain). Lithium nitrate (99.995%) was supplied by Merck (Darmstadt, Germany). A multi-elemental ICP standard solution (1000 mg L^{-1}) containing Ag, Al, B, Ba, Bi, Ca, Cd, Co, Cr, Cu, Fe, Ga, In, K, Li, Mg, Mn, Na, Ni, Pb, Sr, Tl, and Zn was obtained from Sigma-Aldrich (Steinheim, Germany).

2.2 Samples

To assess the applicability of MICAP-OES for the quality control LiBs related materials, 6 raw materials commonly employed in cathode manufacturing processes were analysed to evaluate potential matrix effects and elemental recovery during sample preparation. All the materials employed were of battery-grade quality and were obtained from different distributors. The analysed materials were: (i) lithium carbonate (99.9%) (Li_2CO_3); (ii) lithium hydroxide monohydrate (99.995%) ($LiOH \cdot H_2O$); (iii) cobalt (II) sulphate heptahydrate (99%) ($CoSO_4 \cdot 7 H_2O$); (iv) manganese (II) sulphate monohydrate (98%) ($MnSO_4 \cdot H_2O$);

(v) nickel (II) sulphate hexahydrate (98%) ($NiSO_4 \cdot 6\ H_2O$); and (vi) iron (III) phosphate dihydrate ($FePO_4 \cdot 2\ H_2O$). The inclusion of these precursors provides a representative overview of the elemental profiles encountered prior to cathode synthesis.

In addition, 10 cathode samples, including a cathode Certified Reference Material (CRM) (i.e. NMC111 BAM S014), a cathode Candidate Certified Reference Material (NMC811, $LiNi_{0.8}Mn_{0.1}Co_{0.1}O_2$) and different cathode samples of lithium transition metal oxides, were selected to represent a wide range of compositions and manufacturing sources. The composition of the different cathodes selected was: (i) three Li-based cathode with different chemistries, including lithium iron phosphate (LFP, $LiFePO_4$), lithium manganese oxide (LMO, $LiMn_2O_4$) and lithium nickel cobalt aluminium oxide (NCA, $LiNi_{0.8}Co_{0.15}Al_{0.05}O_2$); (ii) one lithium cobalt oxide (LCO, $LiCoO_2$); and (iii) five lithium nickel manganese cobalt oxides (NMCs) of varying stoichiometries— NMC111 ($LiNi_{0.33}Mn_{0.33}Co_{0.33}O_2$), NMC442 ($LiNi_{0.4}Mn_{0.4}Co_{0.2}O_2$), NMC532 ($LiNi_{0.5}Mn_{0.3}Co_{0.2}O_2$), and NMC622 ($LiNi_{0.6}Mn_{0.2}Co_{0.2}O_2$). All of these samples, with the exception of both CRMs obtained from the Federal Institute for Materials Research and Testing (BAM), were acquired from various distributors.

2.3 Sample preparation

All samples were digested in triplicate using a Ultrawave oven (Milestone s.r.l., Sorisole, Italy) according to the manufacturer's recommendations adapting the conditions defined in the Chinese standard protocols[5,6,7,8,9,10,11,12,13,14,15,16] (Tables S1 in the Supplementary material). For raw materials, 0.15 g of sample

were digested with 4 mL of HNO_3 69% w w^{-1}, except for $FePO_4$ for which 4 mL of HCl 37 % w w^{-1} were used instead (Table S2). As regards cathode materials, 0.15 g of each sample were digested with 4 mL of aqua regia (1 mL of HNO_3 69% w w^{-1} 4 mL of HCl 37 % w w^{-1}) (Table S3). After the digestion process samples were transferred to polyethylene bottles and brought to a final weight of 15 g with ultrapure water. Finally, the digested raw materials and cathodes were brought to a 1:100 and 1:200 dilution, respectively, with ultrapure water following the Chinese standard protocol recommendations (Tables S1). Samples were stored at 4 ºC until analysis by MICAP-OES.

2.4 Matrix and analyte solutions

Multielemental solutions containing 10 mg kg^{-1} of each analyte were formulated in synthetic matrices designed to replicate the elemental composition of both raw materials and cathodes sample digests following the Chinese standards protocols recommendations (Table 1). These solutions were used to investigate spectral and non-spectral interferences arising from the main constituents (i.e., Co, Fe, Li, Mn and Ni) commonly found in these type of samples (a detailed discussion on interferences is provided in sections 3.1 and 3.2). For comparison purposes, a 5% w w^{-1} nitric acid solution was employed as a reference matrix.

Table 1. Composition of major elements remaining in both raw and cathode materials digests.

	Composition after digestion (mg kg^{-1})

	Material	Li	Co	Mn	Ni	Fe
Raw materials	Li_2CO_3	1900	-	-	-	-
	LiOH	1700	-	-	-	-
	$CoSO_4$	-	2100	-	-	-
	$MnSO_4$	-	-	3220	-	-
	$NiSO_4$	-	-	-	2200	-
	$FePO_4$	-	-	-	-	3000
Cathodes	LFP	250	-	-	-	1800
	LCO	375	3000	-	-	-
	LMO	200	-	2900	-	-
	NCA*	350	600	-	2750	-
	NMC111	375	1000	930	1000	-
	NMC442	375	600	1125	1200	-
	NMC532	375	600	850	1500	-
	NMC622	375	600	550	1775	-
	NMC811	375	300	275	2350	-

*75 ppm of aluminium.

2.5 MICAP instrumentation

Elemental analyses were carried out using a MICAP-OES 1000 device (Radom Corporation, Pewaukee, USA), whose technical specifications have been detailed in prior studies. [28,29,30,31,] The sample introduction system employed consisted of a OneNeb® pneumatic nebulizer (Ingeniatrics, Sevilla, Spain) coupled to a cyclonic spray chamber. This sample introduction system combination was selected to minimize the possible matrix effects caused on aerosol generation and transport.[28,29] All the operating conditions and the emission lines employed through this work, with information about the upper electronic level involved in each electron transition ($E_{upper\ level}$), are gathered in Table S4 and Table S5, in the Supplementary material, respectively.

3. Results and discussion

As it was previously mentioned, China has proposed the first set of standard protocols to ensure the quality of LiBs related materials, which specify the maximum impurity content (i.e., Al, B, Ca, Cd, Co, Cr, Cu, Fe, Mg, Mn, Na, Ni, Pb, Zn) and the concentration of major elements (Co, Fe, Li, Mn, Ni). These standard procedures include a series of recommendations for sample pretreatment for raw materials and the LCO cathode. However, no information is provided for other type of cathodes (LFP, LMO, NCA and NMCs). Therefore, raw materials and LCO were digested according to Chinese standards procedures (adapted conditions in Table S2) whereas the remaining samples were pretreated according to the procedures recommended by MW oven manufacturer (Table S3). With the aim of assessing both spectral and non-spectral interferences as well as optimizing MICAP-OES operating conditions, different analyte synthetic solutions simulating the compositions indicated in Table 1 were used. For the sake of comparison, a 5% w w^{-1} nitric acid solution was used as reference.

3.1 *Spectral interferences*

To evaluate possible spectral interferences, the full spectrum (wavelength range between 194-625 nm) was registered operating all the matrix solutions gathered in Table 1 and compared with that obtained for the reference solution, 5% w w^{-1} HNO$_3$ (Fig. S1). The simplest background was obtained for the lithium solutions regarding the emission signal obtained operating the reference solution since its main emission lines were specifically located at 550-600 nm wavelength

range. Conversely, more complex backgrounds were obtained for the rest of the matrices due to the appearance of the different atomic and ionic emission lines of the major elements (i.e., Co, Fe, Mn, Ni) present in those solutions. However, non-significant spectral interferences were detected for the most sensitive emission lines selected for the impurity elements (i.e., Al, B, Ca, Cd, Co, Cr, Cu, Fe, Mg, Mn, Na, Ni, Pb, Zn) (Table S2) except for Pb I 405.781 nm, which is interfered by the Mn I 405.795 nm line in the matrices with higher Mn concentration (i.e., the $MnSO_4$ raw material and the LMO cathode) (Figure S2). Alternatively, the second most sensitive emission line (Pb I 368.346 nm) could be employed since it is not interfered. Consequently, the determination of Pb may be compromised by the reduced sensitivity of this line for samples with more restrictive regulatory limits (e.g., on the order of a few mg kg^{-1}).

3.2 Non-Spectral interferences

To date, most studies on non-spectral interferences in MICAP-OES have focused on alkali and alkali earth elements (Li, Na, Ca, etc.)[26,30] and no information is available about matrix effects by transition metals. In this study, for the first time, the influence of the major elements present in LiB related materials (i.e., Co, Fe, Mn and Ni) on both the nebuliser gas flow rate (Q_g) and the atomic and ionic emission signals of the spectral lines of the different elements regulated by the Chinese standard protocols was evaluated individually and in combination, including mixtures containing high concentrations of Li.

3.2.1 Influence of the nebulizer operating conditions

As previously reported in the literature, the influence of Q_g in high-power (N_2)-cavities depends on the emission line considered and the nature of the matrix employed.[30,31] Thus, the influence of Q_g for a total of 36 emission lines was evaluated operating the different matrices selected. Fig. 1 shows the influence of Q_g on the net emission signal obtained for Mg I 285.213 nm (Fig. 1A, C and E) and Mg II 280.270 nm (Fig. 1B, D and F) for the different matrices evaluated (raw materials and cathodes) and the reference solution. Both emission lines have been selected to show the general behaviour observed when operating the matrices evaluated in this work. The results obtained for the rest of the emission lines are included in the supplementary material (Fig. S3). As it can be observed, the atomic emission for all the matrices shown an increase with Q_g up to 0.9 L min^{-1} (Fig. 1A, C and E). In the case of ionic emission, the signal obtained for the matrices related with the raw materials (Fig 1B) exhibited, in general, a plateau at Q_g 0.5 L min^{-1}, with the exception of the Li 1900 mg kg^{-1} matrix, for which the emission signal decreased from this Q_g onwards. For the cathode matrices (Fig. 1D and F), this plateau was reached at Q_g 0.7 L min^{-1}. Similar findings were obtained for the remaining emission lines evaluated (Fig. S3). These results are similar to those previously reported for MICAP-OES operating saline solutions (i.e., 0.1 mol L^{-1} Na, 0.25 mol L^{-1} Ca, and 0.03 mol L^{-1} K) and prove that, unlike other high-power (N_2)-cavities, MICAP-OES showed a good tolerance working with matrices that present a high concentration of total dissolved solids.[30,31] In fact, after running the instrument for several hours (>5 h), no significant salt deposits were noticed within the torch. Consequently, considering the results described and in order to measure both atomic and ionic emission lines in the

same run to maximise the sample throughput, a Q_g 0.9 L min^{-1} was selected as a common condition.

In agreement with previous studies in the literature, different behaviours were registered as a function of the emission line characteristics. For atomic emission lines (Fig. 1A, C and E), no significant changes were registered for any of the matrices evaluated regarding the reference solution, with the exception of the Li 1900 mg kg^{-1} matrix, for which a 1.6-fold increase in the emission signal, approximately, was registered for Mg I 285.280 nm at Q_g 0.9 L min^{-1}. Conversely, for the Mg II 280.270 nm, the emission signal was found to be negatively affected in the presence of the different matrices evaluated with respect to the reference solution (Fig. 1B, D and F). For instance, when operating raw material-based solutions at Q_g 0.9 L min^{-1}, ionic emission was reduced by approximately 20% for the Co, Fe, Mn and Ni matrices, and a 60% for the Li matrix regarding the reference solution. However, a 30% decrease in the emission signal was observed for cathode-based solutions These behaviours are similar to the data previously reported operating saline matrices (0.1 mol L^{-1} Na, 0.25 mol L^{-1} Ca, and 0.03 mol L^{-1} K) in MICAP-OES,[30] but contrary to those reported by Hallwirth et al.,[26] who encountered signal decrease for both atomic and ionic emission lines when operating a 50 mg kg^{-1} Li solution. The origin of these discrepancies is not clear, but it is likely related to the different experimental setup (i.e., nebulizer and spectrometer design) and working conditions employed in both works.[30]

3.2.2 Influence of the wavelength characteristics

As can be deduced from the data obtained and the conclusions drawn in

previous studies on matrix effects using different high-power (N_2)-MIP cavities,[25,30,32,33] atomic and ionic emission is differently affected by sample concomitants. Therefore, this phenomenon was investigated in more detail for the different matrix solutions (Table 1) and emission lines (Table S2) selected in this work. Fig. 2 shows the values of I_{rel} (i.e., relative signal intensity), defined as the ratio between the net emission signal of an emission line obtained in a given matrix and that obtained when working with the reference one (i.e., 5% w w^{-1} nitric acid), in relation to the $E_{upper\ level}$ of each emission line. The signal repeatability calculated was ~3% RSD (5 replicates), so it can be considered that I_{rel} values below 0.94 or higher than 1.06 (i.e. exceeding an uncertainty range of ± 6%) denote matrix effects.

Journal of Analytical Atomic Spectrometry Accepted Manuscript
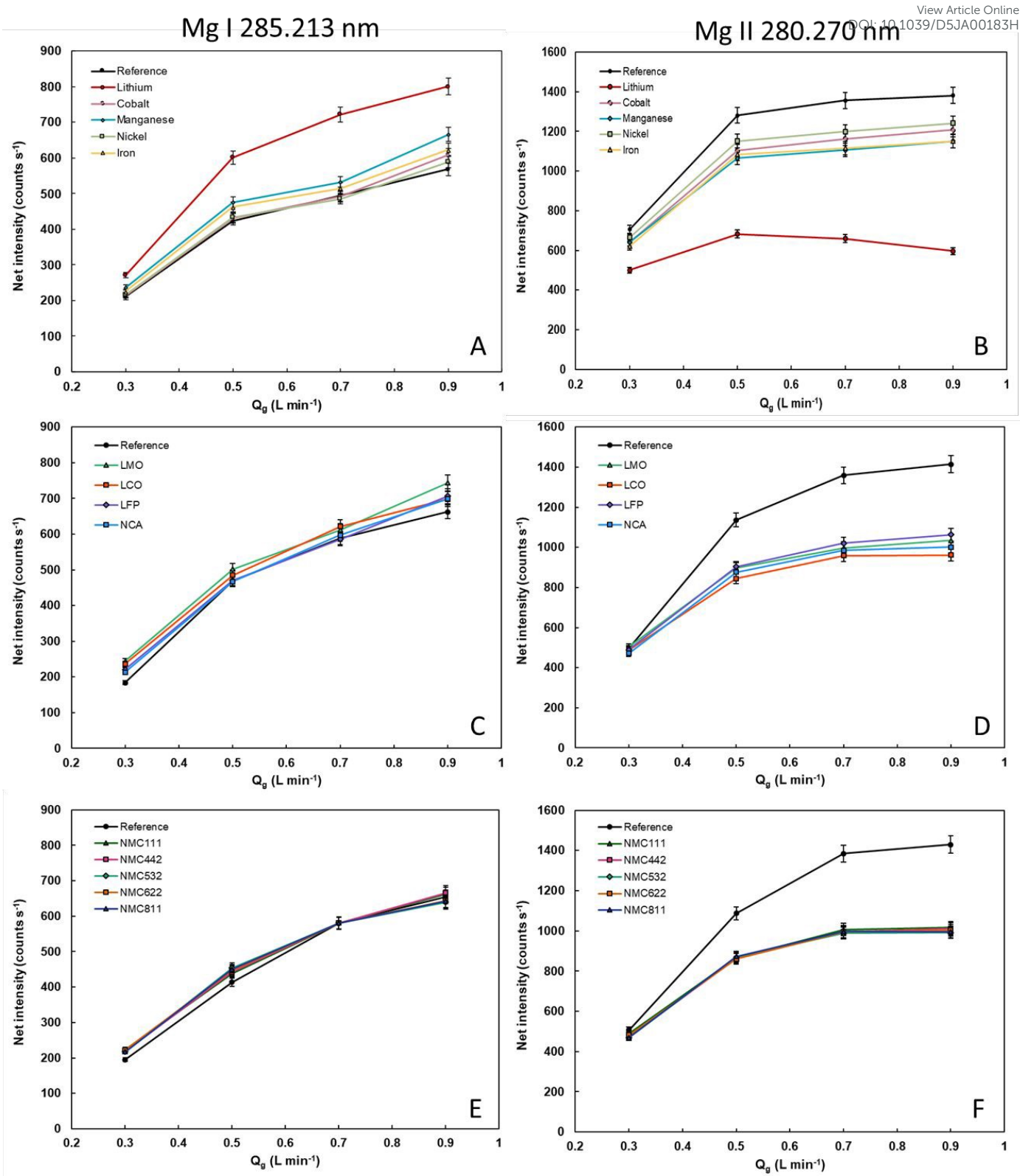
Fig. 1. Influence of the nebulization gas flow rate (Q_g) on the net emission intensity for Mg I 285.213 nm and Mg II 280.270 nm operating the solutions related to raw materials (A and B) and cathodes (C, D, E and F). Q_l 500 µL min^{-1}; TExposure 1000 ms.

In general, all ionic lines evaluated showed negative matrix effects, irrespective of the matrix considered, with particularly pronounced effects registered for the Li matrix. As regards the matrices related with the raw materials (Fig. 2A), the magnitude of the matrix effects increased with the $E_{\text{upper level}}$. In this case, I_{rel} values of approximately 0.94 (0.55 in the case of the Li matrix) were obtained for the least energetic ionic emission lines ($E_{\text{upper level}}$ = 9.2 eV) whereas I_{rel} values as low as 0.75, approximately (up to 0.25 for the Li matrix), were registered for the emission lines with higher $E_{\text{upper level}}$. Conversely, for the cathode matrices (Fig. 2B and C), I_{rel} values range between 0.7-0.8 for all the emission lines evaluated regardless of the matrix.

Regarding atomic emission, no significant changes in the emission signal were observed for the matrices evaluated, with the exception of the Fe, Li and Mn matrices in the case of raw materials, and in certain atomic emission lines in the presence of cathode matrices. In general, positive matrix effects were registered for Fe and Mn with I_{rel} values about 1.15. In contrast, a more complex behaviour was observed for Li since matrix effects depended on the wavelength characteristics with I_{rel} values decreasing as $E_{\text{upper level}}$ increased (Fig. 2A). Indeed, a cross-over point between positive and negative matrix effects was observed. For atomic emission lines with $E_{\text{upper level}}$ < 4.5 eV, positive matrix effects with I_{rel} values up to 1.55 were registered while for the most energetic ones ($E_{\text{upper level}}$ ≥ 5 eV) negative matrix effects were obtained (I_{rel} values up to 0.7). These results contrast to those reported by Hallwirth et al.,[26] who did not

Journal of Analytical Atomic Spectrometry Accepted Manuscript

observe a correlation between the wavelength characteristics of the emission lines and the magnitude of matrix effects caused by Li. However, the trends exhibited in this work are consistent with those reported in previous studies operating saline solutions in MICAP-OES and other high-power (N_2)-MIP cavities.[30,32,33] It is well-known that the introduction of easily ionization elements into the plasma affects to the ion-atom equilibrium due to the increase of the electron number density modifying the different excitation and ionization mechanisms that takes place into the plasma.[25,30,32,33] In the case of the transition metal elements (Co, Fe, Mn and Ni), the data obtained could be explained by taking into account that: (i) their concentration levels in the matrix solutions were approximately 10-fold lower (i.e. between 0.03 and 0.06 mol L^{-1}) than those of Li (0.3 mol L^{-1}) due to the composition of the materials and the higher dilution factor employed for the cathodes (i.e., 1:100 and 1:200 dilution factors for raw materials and cathodes, respectively) according to the Chinese standard protocols; and (ii) that their ionisation potentials are higher (IP: Co 7.88 eV; Fe 7.90 eV; Mn 7.43 eV; and Ni 7.64 eV) than that of Li (IP: Li 5.3 eV). As a result, transition metal elements exhibit a lower ionization degree in the plasma,[34] and consequently, changes in the electron number density are less significant, affecting less to the plasma conditions. Regarding the cathode matrices (Fig. 2B and C), it is interesting to highlight that atomic emission lines for some elements, such as Na I 589.592 nm, Ca I 422.673 nm, Fe I 371.993 nm, Cu I 327.396 nm, Mg I 285.213 nm, and Mg I 518.360 nm, showed slight matrix effects with I_{rel} values about 1.09 and 1.12.

Therefore, as can be deduced from the previous data, the matrix effects and

17

their magnitude depend on the composition of the matrix, that is, the type of the material to be analysed. In the case of the raw materials, whenever there is Li, Mn and Fe in the matrix in high concentration levels (i.e., LiOH, Li_2CO_3, $MnSO_4$ and $FePO_4$ materials), the signal of the ionic emission lines decreases, while for the atomic ones, in general, there is no matrix effects, with the exception of the Li matrix one. In the cathodes, independently of the sample composition, the ionic emission lines are affected along with the following atomic lines Na I 589.592 nm, Ca I 422.673 nm, Fe I 371.993 nm, Cu I 327.396 nm, Mg I 285.213 nm, and Mg I 518.360 nm. Thus, special attention must be paid to the preparation of the calibration standards needed for the analysis of impurities and major elements in the different samples.

3.3 *Calibration strategies*

According to the Chinese standard protocols,[5,6,7,8,9,10,11,12,13,14,15,16] the impurities of interest in both raw materials and cathodes consist of the following elements: Al, B, Ca, Cd, Co, Cr, Cu, Fe, Mg, Mn, Na, Ni, Pb, Zn. For these elements, the most sensitive emission lines in MICAP-OES are mainly atomic, expect for Ca, Fe and Mn whose most sensitive emission line is ionic. Consequently, when analysing impurities in Li_2CO_3, LiOH, $MnSO_4$ and $FePO_4$ raw materials, matrix-matched calibration standards are the optimal strategy to mitigate matrix effects. Conversely, calibration standards prepared in 5% w w^{-1} nitric acid can be employed in the analysis of the $CoSO_4$ and $NiSO_4$ materials, although special attention must be paid to the Ca, Fe and Mn ionic lines. As regards cathode analysis, the most sensitive emission lines for Ca, Cu, Fe, Mn

Journal of Analytical Atomic Spectrometry Accepted Manuscript

and Na (i.e., Cu I 327.396 nm, Ca II 396.847 nm, Fe II 259.940 nm, Mn II 257.610
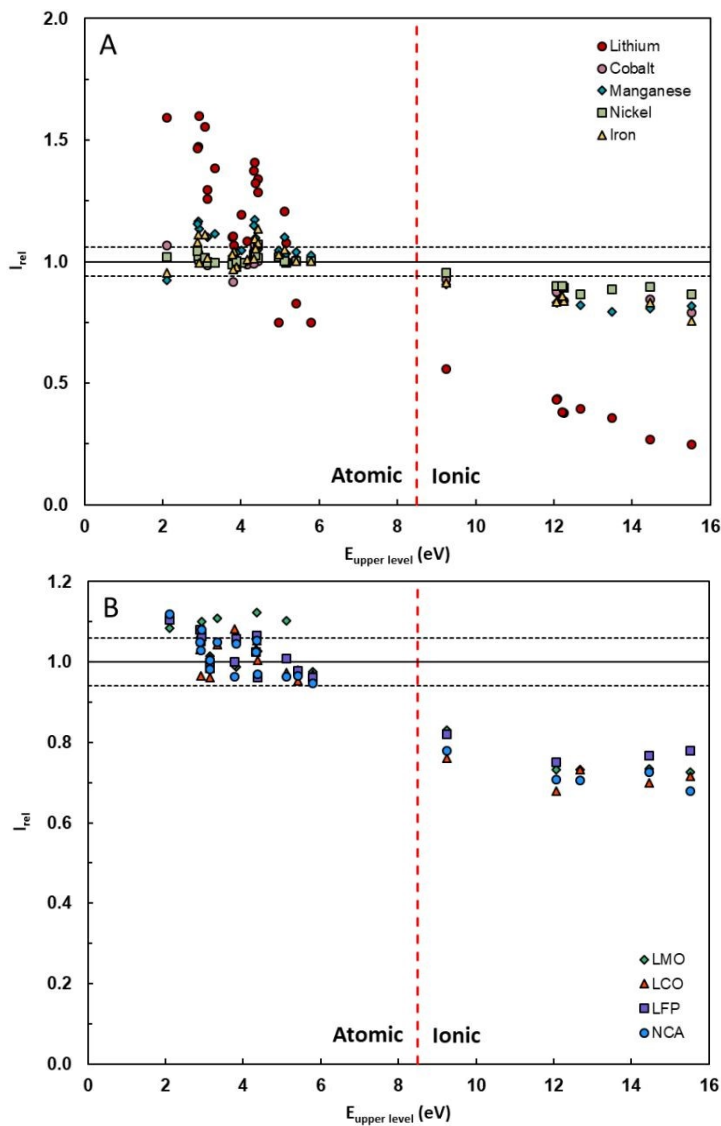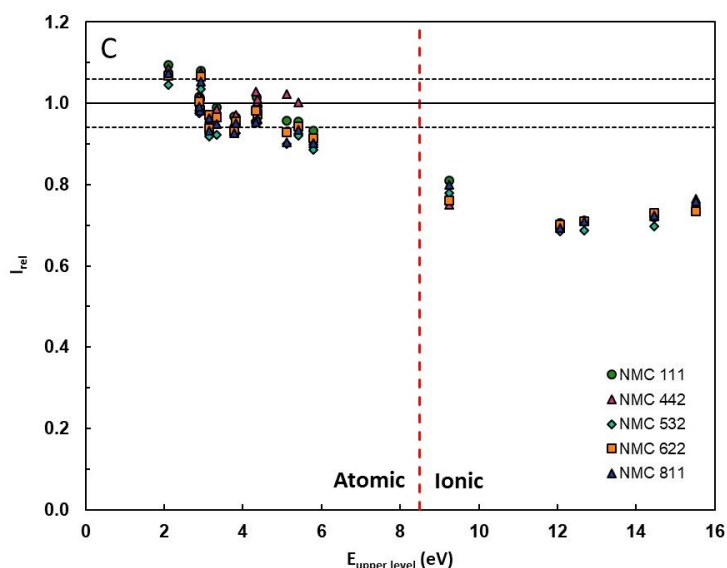
Fig. 2. Influence of the $E_{upper\ level}$ on the I_{rel} operating the solutions related to raw materials (A) and cathodes (B and C) regarding the reference solution (5% w w^{-1} HNO$_3$). Q_l 500 µL min^{-1}; Q_g 0.9 L min^{-1}; TExposure 1000 ms.

nm and Na I 589.592 nm), were interfered irrespective of the solution considered. Therefore, in order to analyse all the impurities simultaneously, matrix-matched calibration standards are recommended. However, if there is no interest in analysing these 5 elements, calibration standards prepared in 5% w w^{-1} nitric acid may be employed.

As indicated in the Chinese regulations, for quality control it is also important to verify the stoichiometry and the content of the major elements (Co, Li, Mn, and Ni) in the cathodes to guarantee the performance of the LiBs. However, given their elevated concentrations in the cathode materials, their analysis is troublesome since the linearity of the most sensitive emission lines is often limited by self-absorption and may even exceed the detector capabilities. It is therefore necessary to apply high dilution factors and, in some cases, to select less sensitive emission lines, to ensure an accurate quantification. In this case, an

optimal dilution factor for cathodes was evaluated to ensure a minimum sample dilution to minimise errors. The minimum dilution factors employed ranged from 1:850 for NMC111, NMC442, NMC532 and NMC622 to 1:800 for the LFP cathode. However, these dilutions are not suitable for the simultaneous analysis of impurities and major elements in these samples, thus two different analyses should be performed instead.

Alternatively, to address the aforementioned issue and carry out the simultaneous analysis of both major elements and impurities in cathodes, the feasibility of reducing the time exposure, and, when necessary, employing less sensitive emission lines was evaluated. This approach aimed to allow sample analysis in a single run without compromising accuracy and improving sample throughput. To this end, the most sensitive emission lines were selected for impurities, whereas two different emission lines were considered for major elements (i.e., the most sensitive line and another with lower sensitivity for some elements such as Co I 345.350 nm, Fe I 371.993 nm, Mn I 322.809 nm, Ni I 300.249 nm). Additionally, two different time exposures within the same run, 1000 ms for impurities and 40 ms for major elements, were selected. This approach was used to ensure that the sensitivity was highly enough for the analysis of impurities and that the major elements were within the dynamic linear range (DLR). In this case, the use of matrix-matched calibration standards was mandatory for all the cathodes. Under these experimental conditions, both impurities and major elements could be analysed satisfactory. Nonetheless, it is important to highlight that with this strategy the relative standard deviation (RSD) of the results was higher regarding the previous one. At lower time exposures,

the DLR increased between 3 to 10-fold for all the major elements (e.g., from 0.3-500 mg kg^{-1} to 0.7-3500 mg kg^{-1} for Co, 0.13-250 mg kg^{-1} to 0.7-2500 mg kg^{-1} for Fe or 0.05-150 mg kg^{-1} to 0.5-500 mg kg^{-1} for Li), but at the same time the RSD obtained increased by a factor of 9 (i.e., from 0.1-1.1% to 3-9%). This fact can be attributed to the lower sensitivity of some of the emission lines selected and the lower period of time that the detector is recording the emission signal. Consequently, in this study, the selected experimental conditions for the determination of both impurities and major elements in the different samples in order to validate the method proposed, consisted in matrix-matched calibration standards, a 1000 ms time exposure, and Q_g 0.9 L min^{-1} and Q_l 500 µL min^{-1} in order to mitigate matrix effects and ensure an accurate analysis of the different elements.

3.4 *Method validation*

To evaluate the feasibility of MICAP-OES for the quality control of raw materials and cathodes from LiBs, a certified reference material (i.e., NMC111 BAM S014) and a wide range of raw materials (e.g., Li_2CO_3, LiOH, $CoSO_4$, $MnSO_4$, $NiSO_4$ and $FePO_4$) and lithium-based cathodes (e.g., LFP, LCO, LMO, NCA, and six NMCs with different stoichiometries) were employed to cover the diversity of materials currently found and used in the LiBs industry.

3.4.1 Limits of detection

The methods limits of detection (mLODs) were calculated from the calibration curve elaborated for each sample (i.e., matrix matched calibration standards and

1000 ms time exposure) according to the IUPAC guidelines and considering the

dilution factors applied to each one.[35] The LODs values obtained, expressed as

mg kg^{-1} of dry weight (n=3), for the elements of interest according to the Chinese

standard protocols for the raw materials and cathodes are gathered in Tables 2

and 3, respectively. In general, the mLOD values for the raw cathodes were

higher than those obtained for the raw materials. This may be due to the different

dilution factors applied for each type of sample. It is interesting to note that the

mLODs for Co, Fe, Li, Mn and Ni in these materials are not relevant as they were

present in high concentrations. According to the Chinese standard protocols

(Table S6), the mLOD values obtained for the raw materials allow the

determination of almost all the impurities regulated in the different materials, with

the exception of Pb and Zn in $CoSO_4$, NiSO4 and Li_2CO_3, as well as, Cd in $NiSO_4$,

Pb in $MnSO_4$, Al, Mn and Ni in Li_2CO_3, and Cu in LiOH. However, in the case of

cathodes (Table S7), it is possible to analyse all the impurities regulated by

means of MICAP-OES as the mLODs values afforded are below the legal

thresholds established. These differences between both types of samples are

due to the impurity limits imposed on the raw materials are more restrictive (i.e.,

in general one order of magnitude lower) compared to those applied to cathodes.

These mLOD data are similar to those reported for ICP-OES in both raw materials

and cathodes considering the different dilution factors employed.[3,17,18,19,21]

Table 2. Method limits of detection (mLODs) expressed as mg kg^{-1} of dry weight (n = 3) in MICAP – OES for the different raw materials analysed. Q_g 0.9 L min^{-1}, Q_l 0.5 mL min^{-1}, TExposure: 1000 ms.

Element	CoSO$_4$	NiSO$_4$	MnSO$_4$	FePO$_4$	Li$_2$CO$_3$	LiOH

Al I 396.152	1.0	1.0	0.6	0.6	1.0	1.0
B I 249.772	2	2	0.7	1.0	2	2
Ca II 396.847	0.04	0.04	0.3	0.14	0.09	0.09
Cd I 228.802	2	2	3	0.4	6	6
Co I 345.350	-	3	3	3	6	6
Cr I 428.973	1.3	1.3	0.6	0.9	1.0	1.0
Cu I 327.396	0.7	0.7	0.6	2	1.4	1.4
Fe II 259.940	2	2	5	-	2	2
Mg I 279.553	0.16	0.16	0.5	0.06	0.13	0.13
Mn II 257.610	1.0	1.0	-	0.4	2	2
Na I 589.592	0.4	0.4	4	0.3	0.4	0.4
Ni I 345.847	4	-	3	3	9	9
Pb I 405.781	4	4	20*	6	6	6
Zn I 213.857	7	7	5	6	3	3

*mLOD value calculated for the emission line Pb I 368.346.

Table 3. Method limits of detection (mLODs) expressed as mg kg^{-1} of dry weight (n = 3) in MICAP – OES for the different cathodes analysed. Q_g 0.9 L min^{-1}, Q_l 0.5 mL min^{-1}, TExposure: 1000 ms.

Element	LCO	LFP	LMO	NCA	NMC111	NMC442	NMC532	NMC622	NMC811
Al I 396.152	9	4	13	5	20	7	13	5	13
Ca II 396.847	3	0.9	12	1.1	9	30	0.3	4	1.1
Cd I 228.802	30	3	30	40	6	30	30	30	20
Cr I 428.973	6	5	50	7	20	7	12	4	7
Cu I 327.396	9	13	13	6	13	2	4	2	13
Fe II 259.940	13	-	30	20	9	7	30	30	30
Mg I 279.553	0.2	3	5	0.7	2	0.9	3	1.3	5
Na I 589.592	2	2	5	7	7	0.7	13	0.7	5
Pb I 405.781	90	40	30*	100	12	30	30	50	30
Zn I 213.857	40	40	20	70	8	40	60	50	20

*mLOD value calculated for the emission line Pb I 368.346.

3.4.2 Accuracy and precision

The accuracy and precision of the method were evaluated through the direct

analysis of a certified reference material (NMC111 BAM S014) analysed in

triplicate (n=3) and recovery tests due to the unavailability of reference materials

for the Li-based cathodes analysed and the raw materials. To this end, the raw

materials and cathodes samples were fortified with the most relevant impurity

elements according to the Chinese standards protocols, at 0.5 mg kg^{-1} of Al, B,

Ca, Cd, Co, Cr, Cu, Fe, Mg, Mn, Na, Ni, Pb, Zn.

As it can be observed in Table S8, the experimental values obtained for the

major elements and impurities agreed with the certified ones and there was no

significant difference for a p-value 0.05, with the exception of Cr. For this element,

the certified value was below the mLODs, so it was not possible to determine its

concentration. Regarding the recovery tests, according to the European

conformity guidelines on the performance of analytical methods[36], the accuracy

of a recovery test is considered successful if the deviation of the experimentally

determined analyte concentration values and the spiked ones does not exceed

the limit ± 10%. Figure 3 shows the recovery values obtained for Li_2CO_3 raw

material and the NMC442 cathode as a representative of the results obtained.

The remaining data are gathered in Figure S4. In general, for raw materials all

the recovery values obtained were quantitative (range between 90 and 110%)

with the exception of Pb for the $MnSO_4$ material. In this case, the most sensitive

emission line of Pb (i.e., Pb I 405.781 nm) is interfered by the Mn I 405.795 nm.

Consequently, the Pb I 368.346 nm line was used as an alternative. Nevertheless,

the LoDs obtained for this line were 0.2 mg kg^{-1}, so it was not possible to carry

out the recovery test for Pb in the $MnSO_4$ material within the spiked conditions

employed. In the case of cathodes, recoveries for the different elements

evaluated were quantitative independently of the composition. Additionally, data obtained with MICAP-OES have been compared with ICP-OES, as a reference technique in elemental analysis. For this purpose, a recovery test was performed by means of an ICP-OES under the same conditions as with MICAP-OES for one of the most complex samples, the NMC442 cathode. The recovery values obtained in this case were also quantitative for the 10 elements evaluated with values ranged between 88.1 ± 1.5 for Al and 105.8 ± 1.56 for Na. Therefore, all these data demonstrated that MICAP-OES is a suitable technique for the quality control of LiBs related materials. Regarding the relative standard deviation, it was within the 0.1–4% range for all the elements evaluated regardless the sample considered. The method reproducibility was evaluated by analyzing three independent replicates of each sample in five different days, and it was lower than 7% for all the samples tested.

Journal of Analytical Atomic Spectrometry Accepted Manuscript
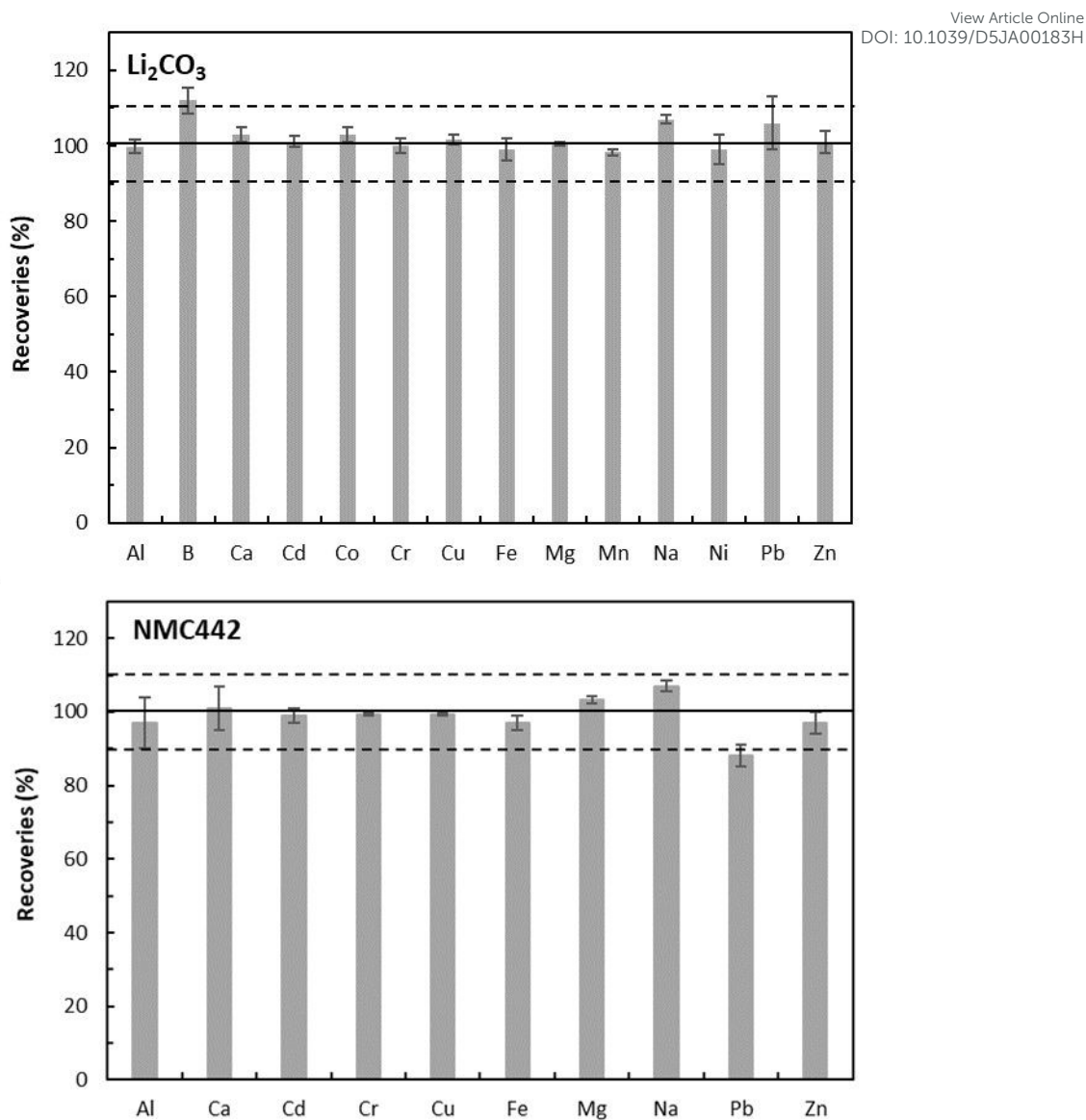
Figure 3. Recoveries expresed as % (mean ± SD, n = 3) obtained for the Li$_2$CO$_3$ raw material and NMC442 cathode analysed by MICAP – OES. Q$_g$ 0.9 L min^{-1}, Q$_l$ 0.5 mL min^{-1}, TExposure: 1000 ms.

3.4.3 Sample analysis

According to Chinese standard protocols, for raw materials, the control of impurities is important to ensure the final quality of the batteries, while for cathodes, both impurities and the stoichiometry of each of the elements that compose them can affect the quality and determine the performance of the

batteries. Therefore, the different LiB related material samples selected have been analysed according to these guidelines. All samples were analysed by means MICAP-OES after digestion. Tables 4 and 5 show the impurities concentration levels found for the raw materials and both, the major elements and impurities determined for cathodes, respectively. For raw materials, the content of impurities lied between the limits set by the different Chinese standard regulations for half of the samples analysed, while the content of B, Cu and Mn for Li_2CO_3, Cu and Mn for LiOH, and Zn for $NiSO_4$ were higher than the less restrictive limits defined according to the characteristics of each material and its use (Table S6). It is interesting to note that, although the impurity values obtained for $MnSO_4$ were below the mLODs, all the elements would be below the specified limits defined for this raw material according to the Chinese standard protocols, with the exception of Pb. The mLOD obtained for Pb (i.e., 20 mg kg^{-1}) with the emission line employed (Pb I 368.346 nm), was higher than the limit set in the regulation (10 or 15 mg kg^{-1}). Consequently, an alternative technique such as ICP-MS would be required to accurately determine Pb in this raw material, due to its superior sensitivity and low detections limits.

In the case of the cathodes, for impurities it can be observed that for 3 of the NMC cathodes (i.e., NMC532, NMC622 and NMC 811) the Zn concentration level found lied out of the limit defined (300 mg kg^{-1}) (Table S7). Regarding the stoichiometry of the main elements, the LCO and LMO samples did not fulfil the requisites of the regulations (Table S9) since the Co concentration in LCO was lower than the established content (i.e., 57-60%), and Li in the LMO cathode was higher than the allowed concentration (i.e., 4.2 ± 0.4 mg kg^{-1}).

Table 4. Impurity content in mg kg^{-1} (mean ± SD, n = 3) in the different raw material samples analysed by MICAP – OES. Q_g 0.9 L min^{-1}, Q_l 0.5 mL min^{-1}, TExposure: 1000 ms.

Element	CoSO$_4$	NiSO$_4$	MnSO$_4$	FePO$_4$	Li$_2$CO$_3$	LiOH
Al I 396.152	< 1	< 1	< 0.6	< 0.6	20.2 ± 0.4	< 1
B I 249.772	< 2	< 2	< 0.7	10.1 ± 0.2	60.1 ± 1.2*	40.5 ± 0.4
Ca II 396.847	10.1 ± 0.3	10.2 ± 0.2	< 0.3	7.23 ± 0.14	40 ± 2	8.6 ± 0.4
Cd I 228.802	< 2	< 2	< 3	< 0.4	< 6	< 6
Co I 345.350	-	500 ± 10	< 3	< 3	< 6	< 6
Cr I 428.973	< 1.3	< 1.3	< 0.6	4.3 ± 0.1	< 1	< 1
Cu I 327.396		< 0.7	< 0.6	30 ± 2	24.2 ± 0.5*	18 ± 2*
Fe II 259.940	< 2	-	< 5	-	< 2	< 2
Mg I 279.553	3.93 ± 0.06	170 ± 3	< 0.5	2.9 ± 0.1	8.1 ± 0.2	3.1 ± 0.4
Mn II 257.610	< 1	< 1	-	500 ± 10	16.5 ± 0.3*	14.6 ± 0.4*
Na I 589.592	2.21 ± 0.12	190 ± 4	< 4	60.5 ± 1.2	100 ± 2	30.2 ± 0.4
Ni I 345.847	< 4	-	< 3	< 3	< 9	< 9
Pb I 405.781	< 4	< 4	< 20	< 6	< 6	< 6
Zn I 213.857	< 7	300 ± 6*	< 5	50 ± 2	< 3	< 3

*The values marked in red are outside the limits stablished in the Chinese standard protocols.[5,6,7,8,9,10]

Table 5. Major (in %) and impurity content (in mg kg^{-1}) (mean ± SD, n = 3) in the different cathodes samples analysed by MICAP – OES. Q_g 0.9 L min^{-1}, Q_l 0.5 mL min^{-1}, TExposure: 1000 ms.

Element	LCO	LFP	LMO	NCA	NMC111	NMC442	NMC532	NMC622	NMC811
Al I 396.152	-	-	-	0.9 ± 0.2	-	-	-	-	-
Co I 240.725	50 ± 4*	-	-	8.53 ± 0.07	20.3 ± 1.0	12.21 ± 0.12	11.96 ± 0.12	11.75 ± 0.09	6.92 ± 0.03
Fe I 371.993	-	36.77 ± 0.14	-	-	-	-	-	-	-
Li I 610.364	7.5 ± 0.3	3.97 ± 0.02	7.85 ± 0.08*	6.79 ± 0.17	6.9 ± 0.3	8.27 ± 0.09	7.48 ± 0.08	7.91 ± 0.04	7.69 ± 0.06
Mn I 280.106	-	-	59.4 ± 0.7	-	16.0 ± 1.0	21.9 ± 0.2	16.11 ± 0.15	10.71 ± 0.09	3.01 ± 0.02
Ni I 300.249	-	-	-	47.3 ± 0.5	20.2 ± 1.0	24.6 ± 0.3	28.9 ± 0.3	35.4 ± 0.3	47.8 ± 0.3
Al I 396.152	1835 ± 9	45.8 ± 0.3	69 ± 4	-	< 20	65.6 ± 0.9	52 ± 2	1170 ± 50	941 ± 4
Ca II 396.847	26 ± 3	51 ± 6	276.9 ± 0.8	86 ± 8	49.4 ± 0.9	17 ± 3	235 ± 3	91 ± 3	21 ± 4
Cd I 228.802	16.4 ± 1.0	< 3	< 30	< 40	< 6	< 30	< 30	< 30	< 20
Cr I 428.973	< 6	21 ± 2	< 50	< 7	< 20	< 7	< 12	< 4	< 7
Cu I 327.396	< 9	40 ± 4	17.1 ± 1.9	15 ± 2	48.1 ± 0.6	< 2	25.0 ± 1.0	18.6 ± 1.5	15 ± 2
Fe II 259.940	34 ± 3	-	37 ± 4	11.6 ± 0.7	< 9	< 7	58.4 ± 0.9	51.3 ± 0.8	55 ± 3
Mg I 279.553	1651 ± 12	25.4 ± 0.3	51.5 ± 1.1	178 ± 2	21.2 ± 0.8	40.4 ± 0.9	161.9 ± 1.0	113.08 ± 0.04	35.3 ± 0.3
Na I 589.592	98 ± 4	45.0 ± 1.3	214 ± 14	15.7 ± 1.3	89.1 ± 1.1	96 ± 6	55 ± 2	99.8 ± 1.9	40 ± 2
Pb I 405.781	< 90	140 ± 10	< 30	< 100	< 12	< 30	< 30	< 50	< 30
Zn I 213.857	< 40	95 ± 7	14.5 ± 1.3	< 70	< 8	215.0 ± 0.2	332.56 ± 0.08*	317 ± 3*	408 ± 15

*The values marked in red are outside the limits stablished in the Chinese standard protocols.[11,12,13,14,15,16]

4. Conclusions

In this study, a novel analytical methodology is proposed for the quality control of LiBs industry materials (i.e., raw materials and cathodes) by means of MICAP-OES in accordance with the available regulations. Both impurities and major elements can be simultaneously determined in a single run by the appropriate selection of operating conditions and the calibration strategies (i.e., matrix-matched calibration standards and lower time exposures). Special care is required for Pb determination in Mn-containing matrices due to the spectral interference of Mn on the most sensitive Pb wavelength. Although the method remains susceptible to matrix effects caused by sample concomitants (mainly Li), changes in both atomic and ionic emission can be satisfactorily corrected using matrix-matched calibration standards. Moreover, the analyte figures of merit shown by MICAP-OES are comparable to those afforded by ICP-OES, making it a suitable technique for quality control applications within LiB related materials. Finally, it is important to highlight that, according to the results discussed, the proposed methodology could also be extended to the quality assessment of materials recovered from LiB-based black mass, supporting its relevance in both manufacturing and recycling contexts.

Conflict of interest

The authors declare that they have no known competing financial interests or personal relationships that could have appeared to influence the work reported in this paper.

Data availability statement

The data supporting this article have been included as part of the Supplementary Information.

References

[1] S. Nowak and M. Winter, *J. Anal. At. Spectrom.*, 2017, **32**, 1833.

[2] A. M. Theodore, J. Chem. Res., 2023, **47**. doi.org/10.1177/17475198231183

[3] J. He, X. Li, F. Wang, M. Jing, and J. Cui, *Thermo Fisher application note*, **73872**.   (Last access March 2025). https://assets.thermofisher.com/TFS-Assets/CMD/Application-Notes/an-73872-icp-oes-elements-lithium-batteries-an73872-en.pdf

[4] H. H. Heimes, A. Kampker, A. vom Hemdt, K. D. Kreisköther, S. Michaelis, and E. Rahimzei, Manufacturing of Lithium-ion battery cell components, RWTH AACHEN University, 2019. ISBN: 978-3-947920-07-5.

[5] Non-Ferrous metal industry standard of the people's republic of china, Battery

grade Lithium carbonate, YS/T 582-2023, 2023.

6 National Standard of the people's republic of china, Battery grade lithium hydroxide monohydrate, GB/T 26008-2020, 2020.

7 Chemical industry standard of the people's republic of china, Cobalt sulfate for battery materials, HG/T 5918-2021, 2021.

8 Industry standard of the people's republic of china, Manganese sulfate for battery materials, HG/T 4823-2015, 2015.

9 Chemical industry standard of the people's republic of china, Nickel sulfate for battery materials, HG/T 5919-2021, 2021.

10 Industry standard of the people's republic of china, Iron phosphate for batteries, HG/T 4701-2021, 2021.

11 Non-Ferrous metal industry standard of the people's republic of china, Lithium nickel cobalt manganese oxide, YS/T 798-2012, 2012.

12 National Standard of the people's republic of china, Lithium cobalt oxide, GB/T 20252-2014, 2014.

13 Non-Ferrous industry standard of the people's republic of china, Lithium iron phosphate, YS/T 1027-2015, 2015.

14 National Standard of the people's republic of china, Lithium nickel manganese oxide, GB/T 37202-2018, 2018.

15 Non-Ferrous metal industry standard of the people's republic of china, Lithium manganese oxide, YS/T 677-2016, 2016.

16 Non-Ferrous metal industry standard of the people's republic of china, Lithium nickel cobalt aluminum oxide, YS/T 1125-2016, 2016.

17 Y. Qi and N. Drvodelic, *Agilent application note*. (Last access March 2025). www.agilent.com/cs/library/applications/an-lithium-carbonate-5800-icp-oes-5994-6112en-agilent.pdf.

18 Spectro analytical instruments, *Spectro application note*. (Last access March 2025). www.spectro.com/landingpages/icp-oes-arcos-application-analysis-of-lithium-composite-oxide-cathode-materials.

19 F. Wenkun, and N. Yingping, *Agilent application note*. (Last access March 2025).https://www.agilent.com/cs/library/applications/application_lithium_impurities_icp-oes_5110_5991-9506en-us-agilent.pdf

20 A. Suárez, A. Jara, R. Castillo, and K. Gallardo, ACS Omega, 2024, **9**, 20129 – 20134.

21 S. Sengupta and D. Kutscher, *Thermo Fisher application note*, **001178**. (Last access March 2025). https://assets.thermofisher.com/TFS-Assets/CMD/Application-Notes/an-001168-tea-icp-oes-icap-pro-xp-lithium-carbonate-an001168-na-en.pdf

22 L. Fu, H. Xie, J. Huang, X. Chen, and L. Chen, Spectrochim. Acta Part B, 2021,

18, 106217.

23 B. M. Fontoura, F. C. Jofré, T. Williams, M. Savio, G. L. Donati, and J. A. Nóbrega, J. Anal. At. Spectrom., 2022, **37**, 966–984.

24 A. Muller, D. Pozebon, and V. L. Dressler, J. Anal. At. Spectrom., 2020, **35**, 2113–2131.

25 R. Serrano, G. Grindlay, L. Gras, and J. Mora, J. Anal. At. Spectrom., 2019, **34**, 1611 - 1617.

26 F. Hallwirth, M. Wolfgang, and H. Wiltsche, J. Anal. At. Spectrom., 2023, **38**, 1682–1690.

27 K. A. M. L. Cruz, G. L. Donati, F. R. P. Rocha, and M. C. Hespanhol, Anal. Methods, 2023, **15**, 3675 – 3682.

28 A. J. Schwartz, Y. Cheung, J. Jevtic, V. Pikelja, A. Menon, S. T. Ray, and G. M. Hietje, J. Anal. At. Spectrom., 2016, **31**, 440-449.

29 K. M. Thaler, A. J. Schwartz, C. Haisch, R. Niessner, and G. M. Hieftje, Talanta, 2018, **180**, 25-31.

30 R. Serrano, G. Grindlay, L. Gras, and J. Mora, Talanta, 2024, **271**, 125666.

31 J. Pérez-Vázquez, A. García-Juan, R. Serrano. G. Grindlay, and L. Gras, Microchem. J., 2025, doi: https://doi.org/10.1016/j.microc.2025.113655.

32 R. Serrano, E. Anticó, G. Grindlay, L. Gras, and C. Fontás, Talanta, 2022, **240**,

Journal of Analytical Atomic Spectrometry Accepted Manuscript

123166.

33 Z. Zhang, and K. Wagatsuma, Spectrochim. Acta Part B, 2002, **57**, 1247–1257.

34 R.S. Houk, Anal. Chem., 1986, **58**, 97–105.

35 J. Inczédy, T. Lengyel, A.M. Ure, A. Gelencsér, and A. Hulanicki, IUPAC Analytical Chemistry Division, Compendium of Analytical Nomenclature, third ed., Blackwell, Oxford, 1998.

36 2002/657/EC: Consolidated text: European Commission Decision of 12 August 2002 Implementing Council Directive 96/23/EC Concerning the Performance of Analytical Methods and the Interpretation of Results.

Journal of Analytical Atomic Spectrometry Accepted Manuscript

Data availability statement

The data supporting this article have been included as part of the Supplementary

Information.